Published in final edited form as:
Pharm Res. 2011 May ; 28(5): 1211–1219. doi:10.1007/s11095-011-0372-2.

Diclofenac Enables Prolonged Delivery of Naltrexone Through Microneedle-Treated Skin

Stan L. Banks,
AllTranz, Inc. Lexington, Kentucky, USA

Kalpana S. Paudel,
Department of Pharmaceutical Sciences, College of Pharmacy University of Kentucky 459 Wethington Bldg., 900 South Limestone Street Lexington, Kentucky 40536, USA

Nicole K. Brogden,
Department of Pharmaceutical Sciences, College of Pharmacy University of Kentucky 459 Wethington Bldg., 900 South Limestone Street Lexington, Kentucky 40536, USA

Charles D. Loftin, and
Department of Pharmaceutical Sciences, College of Pharmacy University of Kentucky 459 Wethington Bldg., 900 South Limestone Street Lexington, Kentucky 40536, USA

Audra L. Stinchcomb
AllTranz, Inc. Lexington, Kentucky, USA

Department of Pharmaceutical Sciences, College of Pharmacy University of Kentucky 459 Wethington Bldg., 900 South Limestone Street Lexington, Kentucky 40536, USA

Abstract

Purpose—The purpose of this study was to determine if non-specific COX inhibition could extend pore lifetime in hairless guinea pigs following microneedle treatment.

Methods—Hairless guinea pigs were treated with microneedle arrays ± daily application of Solaraze® gel (3% diclofenac sodium (non-specific COX inhibitor) and 2.5% hyaluronic acid); transepidermal water loss was utilized to evaluate pore lifetime. To examine the permeation of naltrexone, additional guinea pigs were treated with microneedles ± daily Solaraze® gel followed by application of a 16% transdermal naltrexone patch; pharmacokinetic analysis of plasma naltrexone levels was performed. Histological analysis was employed to visualize morphological changes following microneedle and Solaraze® treatment.

Results—Animals treated with microneedles + Solaraze® displayed extended pore lifetime (determined by transepidermal water loss measurements) for up to 7 days. Enhanced naltrexone permeation was also observed for an extended amount of time in animals treated with microneedles + Solaraze®. No morphological changes resulting from microneedle treatment or COX inhibition were noted.

Conclusions—Non-specific COX inhibition is an effective means of extending pore lifetime following microneedle treatment in hairless guinea pigs. This may have clinical implications for extending transdermal patch wear time and therefore increasing patient compliance with therapy.

A. L. Stinchcomb astin2@email.uky.edu.

Keywords

cyclooxygenase; microneedle; micropore; naltrexone

INTRODUCTION

Transdermal delivery allows drugs to reach the systemic circulation while bypassing the gastrointestinal tract, thereby avoiding many of the disadvantages associated with oral drug delivery. Microneedles (MN) are a minimally invasive means of assisting drug transport across the stratum corneum (SC), the outermost layer of the skin that serves as the primary permeation barrier (1). The microneedles create micropores in the SC, thereby enhancing the permeability of the skin and allowing for enhanced drug delivery of a wide array of compounds. Different applications of MN-assisted transdermal delivery have led to increased permeability of various compounds, including desmopressin, insulin, and some vaccines (1–3). A recent study in human subjects demonstrated that therapeutic levels of naltrexone, an opioid antagonist used for treatment of alcohol dependence, were achieved following MN-facilitated delivery, via application of a naltrexone transdermal patch to MN-pretreated skin (a technique commonly referred to as the “poke-and-patch” method) (4).

One drawback to the MN-assisted delivery approach is the skin’s innate ability to heal itself in a short time following creation of the pores. The previously mentioned human study demonstrated that the skin recovers within approximately 48–72 h following MN treatment. Unfortunately, this would hinder the utility of the “poke-and-patch” approach in a clinical setting by limiting the duration of patch wear time and requiring increased patient involvement. Currently, there is little to no data available describing the physiological mechanisms involved in the pore healing process, making this a challenging target in transdermal research.

Prostaglandins and thromboxane A2 are eicosanoids that are involved in the body’s natural inflammation response and have been described in the wound healing process in the skin (5,6). Both types of eicosanoids are formed from the conversion of arachidonic acid into prostaglandin endoperoxide, a process requiring the cyclooxygenase (COX) enzymes. Two isoforms of COX are known, a constitutively expressed form (COX-1) and an inducible form (COX-2). COX-1 is considered a “house-keeping” enzyme and is thought to be involved in normal skin homeostasis, while COX-2 is an immediate early response gene product whose expression is important in response to injury to the skin. These enzymes are important because the nonsteroidal anti-inflammatory drugs (NSAIDs) exert their effects at this step. In rat skin, both non-specific and COX-2 specific inhibition have been shown to cause a significant delay in wound healing (6).

The aim of this study was to increase the lifetime of pores or “micro-wounds” created by MN insertions *in vivo* by treating hairless guinea pigs (GP) with diclofenac, a non-specific cyclooxygenase (COX) enzyme inhibitor, in an attempt to inhibit the inflammatory response that may be involved in pore healing. Transepidermal water loss (TEWL) and pharmacokinetic analysis of GP plasma samples were utilized to monitor pore closure and permeation of a 16% naltrexone HCl (NTX·HCl) gel. Tissue histology was also employed to look for morphological changes following treatment with MNs and diclofenac.

MATERIALS AND METHODS

Materials

NTX·HCl was purchased from Mallinckrodt Inc. (St. Louis, MO, USA). Propylene glycol (PG) was purchased from Sigma Chemical (St. Louis, MO, USA). Formic acid, ethyl acetate, acetonitrile (ACN), isopropanol, hydrochloric acid (HCl), and sodium hydroxide were obtained from Fisher Scientific (Fairlawn, NJ, USA). Natrosol® (Hydroxyethylcellulose250HHX PHARM) was a gift from Hercules, Inc. (Wilmington, DE, USA). Benzyl alcohol was purchased from Spectrum Chemical MFG. Corp. (Gardena, CA, USA).

Preparation of Drug Formulations

Solaraze® gel, containing 3% diclofenac and 2.5% hyaluronic acid (HA), was purchased through the University of Kentucky. Sixteen percent NTX·HCl gel was prepared as described by Wermeling *et al.*; 2.5% HA gel containing PEG 550:H_2O 60:40 was prepared as a control treatment to determine effect of HA alone during TEWL experiments.

Microneedle and Occlusive Patch Covering Preparation

Microneedles and the occlusive patch coverings were prepared as described by Wermeling *et al.* (4). Briefly, using methods described in detail previously, solid MN adhesive patches were fabricated at Georgia Tech for insertion into the skin (7). Fixed MN geometries were cut into 75-μm-thick stainless steel sheets (Trinity Brand Industries, SS 304; McMaster-Carr, Atlanta, GA, USA) using an infrared laser (Resonetics Maestro, Nashua, NH, USA) and were then manually bent perpendicular to the plane of their metal substrate. For better insertion and adhesion of patches to the skin, MN arrays were assembled into adhesive patches as described previously (8). The adhesive served to hold the MNs firmly against the skin by compensating for the mechanical mismatch between the flexible skin tissue and the rigid MN substrate. The MN patches were assembled in a laminar flow hood for cleanliness and then ethylene oxide sterilized (AN 74j, Andersen Sterilizers, Haw River, NC, USA) before use. MN arrays were fabricated to produce patches containing 50 MNs arranged in 5×10 arrays of MNs (Fig. 1). Each MN measured 620 μm in length, 160 μm in width at the base, and less than 1 μm in radius of curvature at the tip.

The transdermal (TD), occlusive protective covering patches of NTX·HCl (6.7 cm^2) were fabricated by sandwiching a rubber ringed barrier to create a reservoir between a drug-impermeable backing membrane (Scotchpak™ #1109 SPAK 1.34 MIL Heat Sealable Polyester Film) and an ARcare® 7396 adhesive around the edge of the rubber spacer. The impermeable backing laminate was adhered to the rubber retaining ringed barrier with ARcare® 7396. Finally, ARcare® 7396 was placed on the bottom of the rubber ringed barrier to maintain intimate contact with the skin and prevent evaporation of the gel formulations. The protective patch was placed on a release liner composed of Scotchpak™ 9742. The circular NTX·HCl patch area slightly exceeded the surface area of MN-treated skin to insure adequate coverage of the micropores and to reduce formulation pooling in square TD patches.

Transepidermal Water Loss Experiments

All experimental procedures were approved by the University of Kentucky IACUC and were in accordance with institutional guidelines. Transepidermal water loss (TEWL) measurements (cyberDerm RG-1 open chamber evaporimeter) (cyberDERM, Media, PA) were used to evaluate pore lifetime following MN treatment. TEWL was chosen as a method of pore viability measurement due to its ability to detect small changes in the rate of water loss through the skin (9–11). Hairless guinea pigs were either treated with two fifty MN

arrays or no MN array. Application of two MN arrays was used to ensure that the sensitivity of the instrument could detect small differences in water loss due to micropores in the skin *versus* water loss from the occluded skin. This had already been determined as the standard number of arrays to be applied to guinea pig skin to measure for water loss (12). Previous work has reported TEWL measurements of non-treated occluded skin as a control; thus, this control was not repeated for these experiments. Non-treated occluded skin will have an elevated TEWL reading due to hydration of the skin surface. However, MN-treated occluded skin will have a higher TEWL reading compared to the non-treated occluded skin until the MN pores close (12).

Approximately 100 μl of Solaraze® or 2.5% HA gel was rubbed into the MN-treated or no-MN control area and covered with an occlusive protective patch covering. On each day of TEWL measurements, the treated areas were dried with sterile gauze, and measurements were made immediately. Re-application of gels was performed each day after TEWL readings were made, and the area was covered with the occlusive patch systems. An initial TEWL reading was made for a baseline level, and then TEWL readings were taken every 24 h. MN-treated and control areas were cleaned before TEWL readings were taken.

Naltrexone Pharmacokinetic Studies With Mn And Solaraze® Treatment

In Vivo Pharmacokinetic Studies—Hairless guinea pigs were treated with one fifty-MN array. Approximately 100 μl of Solaraze® was rubbed into the MN-treated area, and 0.5 mL of 16% NTX·HCl gel was placed on top of the Solaraze® gel and covered with an occlusive protective patch covering. This procedure was repeated daily for seven days to ensure that an adequate amount of diclofenac came into contact with the MN-treated area. For control animals, a one-time application of one fifty-MN array was applied to the GP, one dose (0.5 mL) of 16% NTX·HCl gel was applied to the skin, and a protective covering patch was applied. There was not significant depletion of the drug from the gel, as a similarly done study showed that less than 5% of the total drug applied was delivered through the skin in seven days. After the study, the area was inspected to ensure the gel had maintained contact with the treated area on both control and Solaraze®-treated animals. Blood samples were drawn from surgically placed cannulas in the GPs as described by Paudel *et al.* and stored at −70°C until analysis (13).

HPLC/MS/MS Conditions—The LC-MS/MS system consisted of a Waters Alliance 2695 pump, Alliance 2695 autosampler, and Micromass ZQ detector (Milford, MA) using electrospray ionization (ESI) for multiple ion monitoring. The LC-MS/MS method was modified from Iyer *et al.* (14). Chromatography was performed on a Waters HELIC (2.1×150 mm, 5 μm) column at 30°C with a mobile phase consisting of 0.1% formic acid and ACN at a flow-rate of 0.35 mL/min. The gradient system used began with 95:5 ACN:buffer from 0 to 0.5 min. A linear gradient system ran from 0.5 to 2.0 min until the mobile phase consisted of 100% 0.1% formic acid. This composition was held for 3 min, and then the system was reconditioned for 3.5 min at the initial conditions. The retention time for NTX·HCl was 5.3 min. Electrospray ionization was employed in the positive mode, and the MRM for NTX·HCl was the transition from 342 to 324. The capillary voltage was set to 3.51 V with a cone voltage of 38 V. The source temperature and desolvation temperature were 120°C and 275°C, respectively. Desolvation gas flow was set at 450 L/h, and the cone gas flow was set to 50 L/h. The collision energy to cause the mass transition from 342 to 324 was 30 V.

Guinea Pig Plasma Sample Extraction and Assay Procedure—Samples were prepared and analyzed by a modified method as described by Paudel *et al.* (13). One-hundred μl of plasma was extracted with 500 μl of ethyl acetate. The mixture was vortexed

for 30 s and centrifuged at 10,000× *g* for 20 min. The pellet and supernatant were placed in a −20°C freezer for 15 min to freeze the aqueous pellet. The supernatant was pipetted into a 3 ml glass test tube and evaporated under nitrogen at 37°C. The residue was reconstituted with 100 μl of ACN and sonicated for 15 min. The samples were transferred into auto sampler vials containing low volume inserts, and 20 μl was injected onto the HPLC column. A NTX·HCl standard was first prepared in ACN. A 1 mg/ml stock was diluted to 10 μg/ml and then further diluted to 1000 ng/ml in ACN. From the 1,000 ng/ml stock of NTX·HCl, a final 10, 25, 50, 75, 100, 150 and 250 ng/ml stock solution was prepared. A standard curve of 0.5, 1, 2.5, 5, 7.5, 10, 15, and 25 ng/ml was generated for analysis of NTX·HCl containing 40 ng/ml naloxone as an internal standard. The LOD and LOQ values determined for NTX were both 0.5 ng/ml in acetonitrile; however, the LOQ was determined to be 1.0 ng/ml in plasma, as plasma interference made the blank plasma and 0.5 ng/ml plasma standards indistinguishable by LC-MS/MS. The correlation coefficient for the NTX·HCl calibration curve was r^2=0.99. Similarly, the reproducibility of 6 independently prepared 5 and 10 ng/ml NTX·HCl plasma standards resulted in % RSD's of 7.8% and 5.6%, respectively. Intraday variability of the LC-MS/MS assay was 8.6%RSD.

Histology—At designated time points following MN application and treatment with Solaraze®, GPs were euthanized, and skin was collected for histological analysis. Skin samples containing both dermis and epidermis were fixed in 10% neutral buffered formalin for 24 h. Samples were processed through a series of ethanol dehydrations, saturated with xylene, and paraffin embedded. Paraffin-embedded sections (10 μM) were deparaffinized in xylene and re-hydrated in an ethanol gradient prior to staining with hematoxylin (H) and eosin (E), or using for immunohistochemistry. Antigen detection for immunohistochemistry utilized Vectastain Elite ABC kit (Vector laboratories, Burlingame, CA) and an antibody against COX-1 (Cayman Chemical, Ann Arbor, MI) or 5-bromo-2-deoxyuridine (Invitrogen, Carlsbad, CA). Anti-gens were detected using diaminobenzidine (DAB). For labeling proliferating skin cells, guinea pigs were treated with two IP doses of 100 mg/kg 5-bromo-2-deoxyuridine (Invitrogen) at 24 and 5 h prior to euthanasia and skin collection.

Statistical Analysis—The statistical analysis of data was computed with a Student's *t*-test and one-way ANOVA with post-hoc Tukey's pairwise test using SIGMA-STAT (SPSS, Inc., Chicago, IL, USA) software.

RESULTS

Transepidermal Water Loss Measurements

TEWL is a well-accepted technique for assessing the barrier function of the skin, and it was utilized in this study to determine the lifetime of pores created by MN treatment. Previous data demonstrated that the pores close within 48–72 h under occlusive conditions (without application of any additional treatments, using the same occlusive system and evaporimeter) (4,15); therefore, this study investigated the effect of Solaraze® (3% diclofenac sodium, 2.5% hyaluronic acid) on TEWL measurements, in addition to its effect when combined with MN treatment. Baseline TEWL measurements (prior to applications of any treatment with MNs or Solaraze®) were similar in both groups (12.82±2.9 g/m^2/h for MN-treated site *vs.* 8.5± 1.29 g/m^2/h for non-MN-treated skin). In both groups, TEWL measurements were higher after seven days when compared to baseline. Animals treated with daily application of Solaraze® gel displayed significant differences in water loss (p<0.001) between MN-treated (58.1±1.2 g/m^2/h) and non-MN treated areas (36.5±18.1 g/m^2/h) within each animal after seven days of treatment (Fig. 2), indicating that the increase in water loss was not due to the Solaraze® alone. To rule out any effect of 2.5% HA on pore closure, three GPs were either treated with a 2.5% HA gel + pre-treatment with MNs or with 2.5% HA gel alone. No

significant difference in water loss was noted in the GP skin treated with 2.5% HA gel when in the presence (31.3±6.8 g/m^2/h) or absence (30.5±9.3 g/m^2/h) of MN treatment after three days (p>0.05).

Pharmacokinetic Analysis

In order to complement TEWL measurements, pharmacokinetic analysis was employed to correlate increased pore lifetime with plasma NTX·HCl levels. Fig. 3 displays the plasma levels of NTX·HCl in the hairless guinea pigs (n=4) treated with the combination of MN, Solaraze®, and 16% NTX·HCl gel. Increased plasma levels of NTX·HCl were observed in these animals for seven days (Css = 7.0 ng/mL) when compared to control animals treated with MN and 16% NTX·HCl alone (Css = 3.4 ng/mL for only 2 days) (p<0.05). As a control, four GPs were treated with a one-time application of MNs followed by 0.5 g of 16% NTX·HCl, covering an area of 6.7 cm^2. As seen in Fig. 4, NTX·HCl levels dropped off quickly after 24 h and returned to baseline by 60 h, indicating complete closure of the pores. It can be inferred that the drop in naltrexone levels is due to pore closure rather than depletion of the drug from the gel because a 16% NTX gel would not deplete over the 48–72 h that drug was detected in plasma (assuming that significant effects from depletion can be observed when >10% of drug from formulation is lost). The steady-state concentration of 7.0 ng/ml corresponds to a flux of approximately 16.14 nmol/cm^2/h, and if the Css had remained at 7.0 ng/ml for the entire 72 h profile, this would correspond to total delivery of 2.65 mg of naltrexone. In total, 80 mg of NTX was applied to the MN-treated area; therefore, this 2.65 mg is less than 5% of the dose. All pharmacokinetic parameters are listed in Table 1.

The absolute bioavailability calculation of this prototype patch indicates that approximately 2.5% of the dose passes through the skin. This value is based on the I.V. dose of 3 mg/kg, a systemic dose AUC of 546 ng/ml/h, an 80 mg transdermal dose, and the extravascular dose AUC of 1198.9 ng/ml/h (16). A higher rate of permeation could be achieved from an optimized transdermal system; however, the purpose of this system was to provide a proof of concept dosage form. There is ongoing work to improve the delivery efficiency of the transdermal system.

Histological Evaluation of Skin Following Topical Application of MN and COX Inhibitor

Histological analysis was used to determine whether morphological changes in the skin resulted from application of the MN and COX inhibitor. Separate areas of the skin on the backs of guinea pigs without MN or COX inhibitor (control) were compared to areas treated with MN and COX inhibitor for 24 h, 48 h and 72 h (Fig. 4). There was no observable difference in the thickness of the stratified keratinocyte layer between control treatment and the MN/COX inhibitor treatment at the time-points analyzed. Although the pores formed by the MN application could not be definitively identified in histological sections via this method, analysis of skin sections throughout MN-treated regions identified no evidence of infection or inflammatory cell infiltration.

Analysis of COX-1 Expression and Brdu Incorporation in Guinea Pig Skin

There are significant differences in the cell types which express the COX isoforms in the skin of different species. Immunohistochemistry was utilized to determine the cell types which express COX-1 in the skin of hairless GPs (diminutive hair present, not completely hairless as the name implies). COX-1 expression was concentrated in cells of hair follicles (Fig. 5A filled arrows). The majority of the follicular cells expressing COX-1 showed evidence of expanded cytoplasmic contents with a centralized nucleus, which is characteristic of sebaceous gland cells (17). In addition to the follicular expression, there

was also a lower level of COX-1 expression in the stratified epidermal layer of the skin (Fig. 5A open arrow).

Keratinocyte proliferation may alter the duration of transdermal drug delivery by resulting in the occlusion of the pores formed by MN application. Thus, we examined cellular proliferation using BrdU immunohistochemistry in the hairless GP skin. The majority of cells incorporating BrdU into their nuclei were localized to areas surrounding hair follicles (Fig. 5B filled arrows). The cells composing the stratified epidermal layer of the skin also showed a low level of proliferation (Fig. 5B open arrows). These findings suggest that COX-1 expression is most concentrated in follicles, which is an area of the skin associated with increased cellular proliferation.

DISCUSSION

The advantages of transdermal drug delivery are widely known. However, due to the effective barrier function of the stratum corneum, currently available passive transdermal systems only support the delivery of small, lipophilic drug molecules (1). Microneedles provide an effective means of overcoming these issues by creating pores in the stratum corneum, thereby increasing the permeability of the skin and allowing for a wider array of drugs to be delivered by this route. Microneedle systems are generally well tolerated by patients and are associated with less pain than hypodermic needles (a more traditional approach to bypassing the SC), thus adding to their appeal (1,7,8,18,19).

A transdermal formulation of naltrexone would be optimal for increasing its clinical usefulness in treating opioid and alcohol addiction, though the physicochemical properties of the molecule (specifically its hydrophilicity) prevent it from passing through the skin barrier and achieving therapeutic concentrations. To date, many studies have already been completed in an attempt to increase the hydrophobicity of naltrexone via prodrug methods (20–22). One problem that arises, however, is that the aqueous solubility of naltrexone is desirable to allow the drug to partition into interstitial fluid once it has passed through the skin. This creates a significant challenge for delivering naltrexone via traditional passive transdermal delivery approaches. These properties make naltrexone an excellent candidate for studying MN-enhanced delivery, as the pores created by the microneedles allow naltrexone to pass through the SC, regardless of its hydrophilic nature, where it can readily be measured in plasma via pharmacokinetics with analytical methods previously described (4,23). As noted previously, MN pre-treatment followed by application of a transdermal naltrexone patch leads to higher (and therapeutically relevant) naltrexone plasma levels for up to 72 h in healthy human subjects, demonstrating the effectiveness of the “poke-and-patch” method of MN treatment for delivering naltrexone transdermally (4).

Despite all of the potential advantages of MN-assisted transdermal delivery, the clinical utility of this approach is severely limited by the rapid rates of pore closure. Both animal and human studies have demonstrated that the pores close within 48–72 h (4,15), which would ultimately require more patient involvement with treatment and might potentially negate the positive effects gained by using a microneedle system. Therefore, it is necessary to develop effective means of inhibiting pore closure following MN treatment in order for this type of transdermal delivery to be a realistic clinical tool.

These results have demonstrated that diclofenac, a non-specific COX inhibitor, can contribute to a delay in the pore healing process, indicating a possible role of inflammation in the kinetics of pore closure. As demonstrated by TEWL measurements and steady-state plasma levels of NTX·HCl, pore lifetime was extended to seven days when MN pre-treatment was combined with daily application of diclofenac. Additionally, these data

demonstrated that the 2.5% hyaluronic acid found in the Solaraze® formulation does not have an effect on rates of pore closure, confirming that the effect of Solaraze® gel on pore closure is, in fact, due to the 3% diclofenac sodium. While some concern may be raised about additional risk for infection with extended pore lifetime, the risk is generally considered low following MN treatment, and there were no infections noted in any guinea pigs that were treated with MNs. Occlusive patches were changed daily, and a fresh application of Solaraze® was also applied daily, which reduces the risk of bacterial infection. Additionally, the naltrexone gel formulation contains benzyl alcohol, a bacteriostatic agent with moderate bactericidal properties that helps reduce the risk of infection during the pharmacokinetic studies.

Although diclofenac is a nonselective COX isoform inhibitor, the mechanism resulting in improved MN-assisted transdermal delivery may primarily involve the inhibition of COX-1. The majority of keratinocytes at various stages of differentiation express COX-1, whereas COX-2 is not expressed in normal skin or is limited to a specific stage of keratinocyte differentiation (17,24,25). In models of wound healing, diclofenac administration impairs skin repair because of the inhibition of PGE_2 and/or PGD_2 synthesis that is dependent on the activity of COX-1, but not COX-2 (26). Topical application of PGE_2 or PGD_2 has also been shown to reduce transepidermal water loss following cutaneous barrier disruption in mice (27).

Gross signs of an inflammatory response, characterized by an influx of polymorphonuclear leukocytes or macrophages, are not characteristic of healthy skin. Proliferation is stimulated during the healing of wounds and the inactivation of COX-1 reduces keratinocyte proliferation at the site of wound healing (26). In the current report, we did not identify any evidence of an inflammatory response (characterized by gross cellular infiltration), and COX-1 expression was concentrated around follicles that also stained positive for BrdU incorporation, suggesting that the beneficial effects of diclofenac on improved MN-assisted transdermal delivery may result from inhibiting COX-1-dependent proliferation. This does not, however, eliminate the possibility of less severe inflammation that could not be detected by histological techniques.

CONCLUSION

Non-specific COX inhibition can be utilized in an effort to continually improve MN-enhanced transdermal drug delivery and increase pore lifetime for weekly patch application. Future work should focus on developing a transdermal formulation of naltrexone HCl and diclofenac within a patch system that would deliver a constant daily amount of diclofenac (to maintain pore viability), while not requiring daily application of the diclofenac. Additionally, it would be advantageous to carry out this work with another drug molecule besides naltrexone, to confirm that similar results can also be achieved with MN-assisted delivery of other drugs. Overall, these data demonstrated that improved patient compliance and once-weekly patch application are a realistic goal for the transdermal delivery of naltrexone, and possibly other chemical entities, when combined with MN-pretreatment of the skin.

Acknowledgments

We would like to thank Dr. Harvinder Gill and Dr. Mark Prausnitz at the Georgia Institute of Technology for generously providing the MN arrays used for this work. This work was funded by NIH grant R01DA13425 and AllTranz Inc. ALS and SLB are significant shareholders in AllTranz, Inc., a specialty pharmaceutical company developing COX inhibitor technology for use with microneedles. AllTranz, Inc. and the University of Kentucky have pending patents for this technology.

REFERENCES

1. Prausnitz MR, Langer R. Transdermal drug delivery. Nat Biotechnol. 2008; 26(11):1261–8. [PubMed: 18997767]
2. Prausnitz MR. Microneedles for transdermal drug delivery. Adv Drug Deliv Rev. 2004; 56(5):581–7. [PubMed: 15019747]
3. Arora A, Prausnitz MR, Mitragotri S. Micro-scale devices for transdermal drug delivery. Int J Pharm. 2008; 364(2):227–36. [PubMed: 18805472]
4. Wermeling DP, Banks SL, Hudson DA, Gill HS, Gupta J, Prausnitz MR, et al. Microneedles permit transdermal delivery of a skin-impermeant medication to humans. Proc Natl Acad Sci USA. 2008; 105(6):2058–63. [PubMed: 18250310]
5. Marie, L.; Foegh, PWR. The eicosanoids: prostaglandins, throm-boxanes, leukotrienes, & related compounds. In: Katzung, BG., editor. Basic & clinical pharmacology. 9th ed. McGraw-Hill; New York: 2004. p. 298-312.
6. Futagami A, Ishizaki M, Fukuda Y, Kawana S, Yamanaka N. Wound healing involves induction of cyclooxygenase-2 expression in rat skin. Lab Invest. 2002; 82(11):1503–13. [PubMed: 12429810]
7. Kaushik S, Hord AH, Denson DD, McAllister DV, Smitra S, Allen MG, et al. Lack of pain associated with microfabricated microneedles. Anesth Analg. 2001; 92(2):502–4. [PubMed: 11159258]
8. Martanto W, Davis SP, Holiday NR, Wang J, Gill HS, Prausnitz MR. Transdermal delivery of insulin using microneedles *in vivo*. Pharm Res. 2004; 21(6):947–52. [PubMed: 15212158]
9. Ferguson JC, Martin CJ, Rayner C. Burn wound evaporation—measurement of body fluid loss by probe evaporimeter and weight change. Clin Phys Physiol Meas. 1991; 12(2):143–55. [PubMed: 1855360]
10. Gao S, Singh J. Effect of oleic acid/ethanol and oleic acid/propylene glycol on the *in vitro* percutaneous absorption of 5-fluorouracil and tamoxifen and the macroscopic barrier property of porcine epidermis. Int J Pharm. 1998; 165(1):45–55.
11. Verbaan FJ, Bal SM, van den Berg DJ, Groenink WH, Verpoorten H, Luttge R, et al. Assembled microneedle arrays enhance the transport of compounds varying over a large range of molecular weight across human dermatomed skin. J Control Release. 2007; 117(2):238–45. [PubMed: 17196697]
12. Banks SL, Pinninti RR, Gill HS, Paudel KS, Crooks PA, Brogden NK, Prausnitz MR, Stinchcomb AL. Transdermal delivery of naltrexol and skin permeability lifetime after microneedle treatment in hairless guinea pigs. J Pharm Sci. 2010; 99(7):3072–80. [PubMed: 20166200]
13. Paudel KS, Nalluri BN, Hammell DC, Valiveti S, Kiptoo P, Hamad MO, et al. Transdermal delivery of naltrexone and its active metabolite 6-beta-naltrexol in human skin *in vitro* and guinea pigs *in vivo*. J Pharm Sci. 2005; 94(9):1965–75. [PubMed: 16052561]
14. Iyer SS, Kellogg GE, Karnes HT. A LC-electrospray tandem MS method for the analysis of naltrexone in canine plasma employing a molecular model to demonstrate the absence of internal standard deuterium isotope effects. J Chromatogr Sci. 2007; 45(10):694–700. [PubMed: 18078579]
15. Banks S, Paudel K, Stinchcomb A, Loftin C. COX enzyme inhibitor enables drug delivery through microneedle treated skin for seven days. AAPS J. 2008; 10(S2)
16. Valiveti S, Hammell DC, Paudel KS, Hamad MO, Crooks PA, Stinchcomb AL. *In vivo* evaluation of 3-O-alkyl ester transdermal prodrugs of naltrexone in hairless guinea pigs. J Control Release. 2005; 102(2):509–20. [PubMed: 15653167]
17. Leong J, Hughes-Fulford M, Rakhlin N, Habib A, Maclouf J, Goldyne ME. Cyclooxygenases in human and mouse skin and cultured human keratinocytes: association of COX-2 expression with human keratinocyte differentiation. Exp Cell Res. 1996; 224(1):79–87. [PubMed: 8612694]
18. Haq MI, Smith E, John DN, Kalavala M, Edwards C, Anstey A, et al. Clinical administration of microneedles: skin puncture, pain and sensation. Biomed Microdevices. 2009; 11(1):35–47. [PubMed: 18663579]

19. Mikszta JA, Alarcon JB, Brittingham JM, Sutter DE, Pettis RJ, Harvey NG. Improved genetic immunization via micromechanical disruption of skin-barrier function and targeted epidermal delivery. Nat Med. 2002; 8(4):415–9. [PubMed: 11927950]

20. Hammell DC, Hamad M, Vaddi HK, Crooks PA, Stinchcomb AL. A duplex “Gemini” prodrug of naltrexone for transdermal delivery. J Control Release. 2004; 97(2):283–90. [PubMed: 15196755]

21. Hammell DC, Stolarczyk EI, Klausner M, Hamad MO, Crooks PA, Stinchcomb AL. Bioconversion of naltrexone and its 3-O-alkyl-ester prodrugs in a human skin equivalent. J Pharm Sci. 2005; 94(4):828–36. [PubMed: 15736197]

22. Nalluri BN, Milligan C, Chen J, Crooks PA, Stinchcomb AL. *In vitro* release studies on matrix type transdermal drug delivery systems of naltrexone and its acetyl prodrug. Drug Dev Ind Pharm. 2005; 31(9):871–7. [PubMed: 16305998]

23. Valiveti S, Nalluri BN, Hammell DC, Paudel KS, Stinchcomb AL. Development and validation of a liquid chromatography-mass spectrometry method for the quantitation of naltrexone and 6beta-naltrexol in guinea pig plasma. J Chromatogr B Analyt Technol Biomed Life Sci. 2004; 810(2): 259–67.

24. Scholz K, Furstenberger G, Muller-Decker K, Marks F. Differential expression of prostaglandin-H synthase isoenzymes in normal and activated keratinocytes *in vivo* and *in vitro*. Biochem J. 1995; 309(Pt 1):263–9. [PubMed: 7619067]

25. Buckman SY, Gresham A, Hale P, Hruza G, Anast J, Masferrer J, et al. COX-2 expression is induced by UVB exposure in human skin: implications for the development of skin cancer. Carcinogenesis. 1998; 19(5):723–9. [PubMed: 9635856]

26. Kampfer H, Brautigam L, Geisslinger G, Pfeilschifter J, Frank S. Cyclooxygenase-1-coupled prostaglandin biosynthesis constitutes an essential prerequisite for skin repair. J Invest Dermatol. 2003; 120(5):880–90. [PubMed: 12713596]

27. Honma Y, Arai I, Hashimoto Y, Futaki N, Sugimoto M, Tanaka M, et al. Prostaglandin D2 and prostaglandin E2 accelerate the recovery of cutaneous barrier disruption induced by mechanical scratching in mice. Eur J Pharmacol. 2005; 518(1):56–62. [PubMed: 16000196]

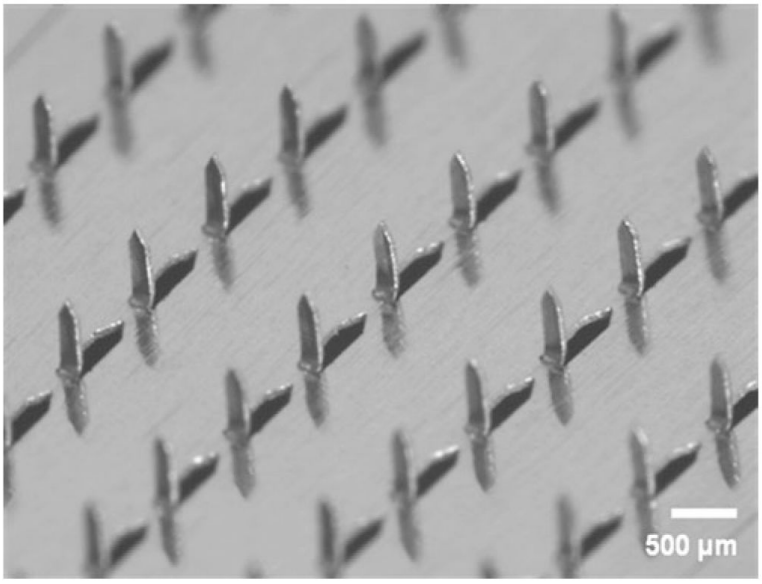

Fig. 1.

Microscopic visualization of the 50 microneedle array, arranged in a 5×10 configuration. Microneedles had the following dimensions: 620 μm in length, 160 μm in width at the base, and <1 μm in radius of curvature at the tip. Photo courtesy of Harvinder Gill and Mark Prausnitz of the Georgia Institute of Technology.

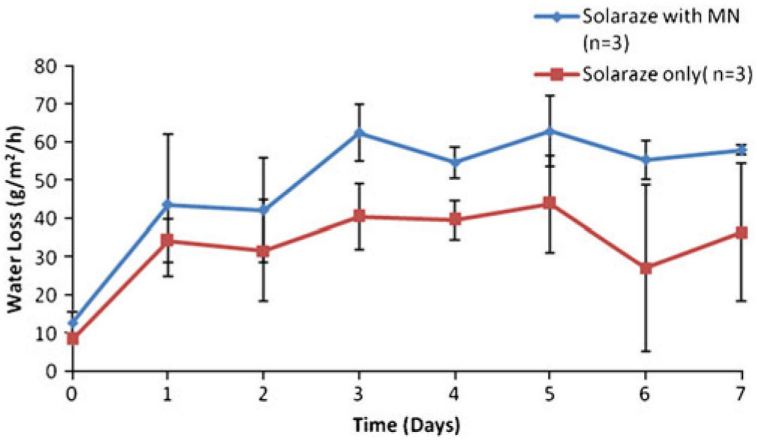

Fig. 2.

Transepidermal water loss readings following daily application of Solaraze® gel to MN-treated skin *vs.* intact skin.

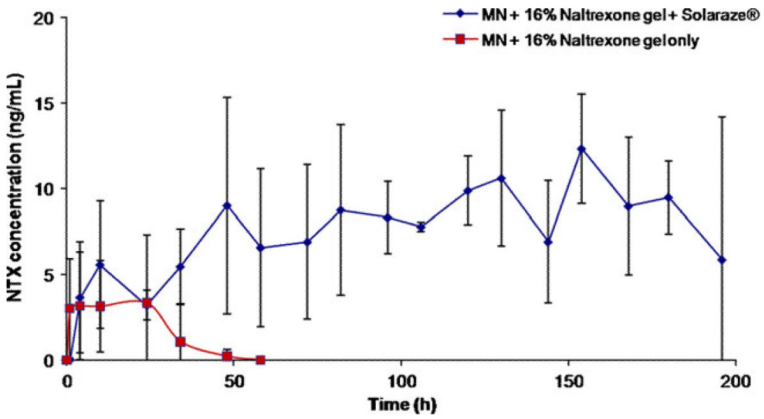

Fig. 3.

Naltrexone plasma profiles after one-time application of MNs in hairless guinea pigs with daily application of 0.5 g of 16% NTX·HCl (control) compared to one-time application of MN +0.5 g of 16% NTX·HCl and approximately 100 μlof Solaraze® topical gel (3% diclofenac sodium), covering 6.7 cm^2 area (n=4).

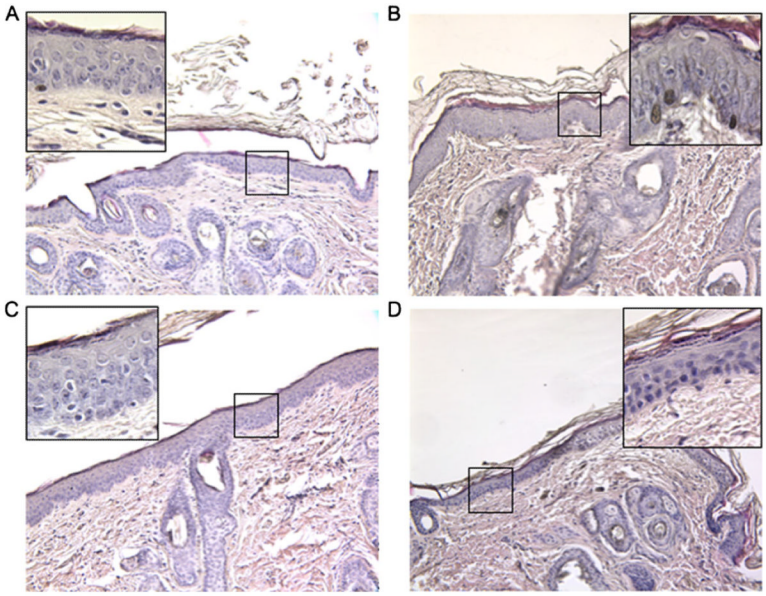

Fig. 4.

Histological analysis of guinea pig skin following COX inhibitor and MN application. Sections of skin stained with H&E prior to COX inhibitor and MN application (**A**), and 24 h (**B**), 48 h (**C**), or 72 h (**D**) following COX inhibitor and MN application.

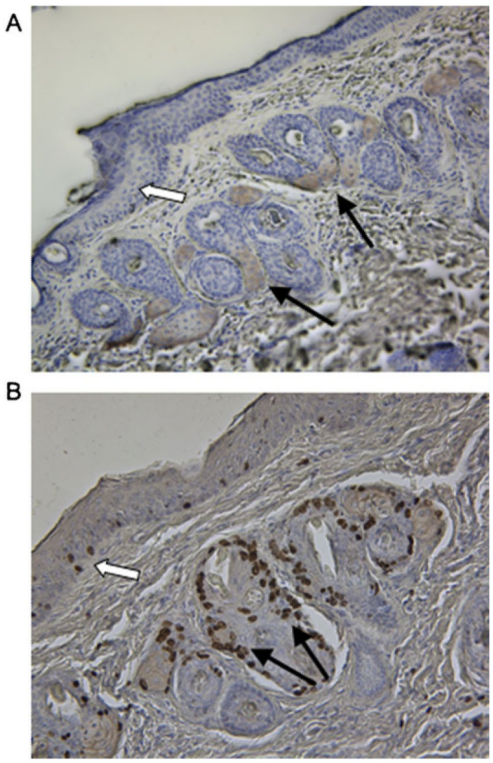

Fig. 5.

Immunohistochemical analysis of COX-1 expression and cellular proliferation in guinea pig skin. (**A**) COX-1 expression concentrated in cells of hair follicles (*filled arrows*) and to a lesser extent in the stratified epithelial layer (*open arrow*). (**B**) The detection of proliferation was concentrated in cells composing hair follicles (*filled arrows*) with a lower level detected in the stratified epithelial layer (*open arrow*). *Brown staining* (DAB reagent) indicates (**A**) COX-1 or (**B**) BrdU detection.

Table I

Pharmacokinetic Parameters of NTX·HCl After One 50-MN Array Application in the Presence or Absence of Solaraze® Gel (n=4 in Each Group)

	MN + Solaraze® + 16% NTX·HCl (*n*=4)	**MN + 16% NTX·HCl (*n*=4)**
C_{ss} (ng/ml)	7.0±1.5	3.4±1.3
C_{max} (ng/ml)	12.9±4.0	7.5±2.5
T_{lag} (h)	21.5±12.6	1.8±1.5
AUC (ng/ml*hr)	1198.9±400.5	258.9±178.7

COX cyclooxygenase, *MN* microneedles, *GP* guinea pig, *HA* hyaluronic acid, *NTX·HCl* naltrexone HCl, *SC* stratum corneum, *TEWL* transepidermal water loss